Minimum-energy point charge configurations on a circular disk

1998 J. Phys. A: Math. Gen. 31 1035

(http://iopscience.iop.org/0305-4470/31/3/014)

J. Phys. A: Math. Gen. **31** (1998) 1035–1047. Printed in the UK PII: S0305-4470(98)83329-5

Minimum-energy point charge configurations on a circular disk

Kari J Nurmela

Helsinki University of Technology, Department of Computer Science and Engineering, PO Box 1100, FIN-02015 HUT, Finland

Received 11 April 1997, in final form 26 September 1997

Abstract. Stochastic global optimization methods are used together with problem-specific heuristics to find configurations of n equal point charges on a circular disk such that the potential energy is minimized. Previous such optimal or conjecturally optimal configurations have been published only for $n \leqslant 23$ and $n = 29, 30, 50$. Earlier results are examined and the best currently known configurations—most of them new—for $n \leqslant 80$ are presented.

1. Introduction

The question: What is the minimum-energy configuration of n equal point charges on a circular disk? was raised in 1985 by Berezin [1]. It appeared that in the optimal configuration not all the charges are located on the disk boundary when $n \geqslant 12$ (for proofs of this fact, see [2–5]). Berezin's original note was followed by a wave of scientific correspondence, where it was discussed whether the charges actually behave 'differently' when they are confined on a circular disk instead of a sphere [6–14].

In [6, 11] it was shown that a (non-optimal) configuration of 17 charges where two charges are placed on the interior of the disk has lower energy than the configuration with 16 charges evenly spaced on the disk boundary and one in the centre of the disk. When the number of charges approaches infinity, the problem tends to the well known problem of charge distribution over a conducting disk [15] with charge density proportional to $(1 - r^2)^{-1/2}$, where r is the distance from the centre of the disk [16, 17].

While no practical applications in physical systems have yet been presented for this kind of minimum-energy configurations, finding minimum-energy configurations is an interesting global optimization problem. It has turned out to be difficult to solve and methods developed for finding optimal charge configurations can probably also be adapted to some other configuration optimization problems.

1.1. Earlier results

The first calculations to find the globally optimal, least energy configurations for $n > 12$ were performed in [18] ($n \leqslant 20$), [16] ($n \leqslant 17$, $n = 29, 30$) and [19] ($n \leqslant 23$, $n = 50$).

Wille and Vennik [19] used a simulated annealing algorithm (see also [20, 21]) and failed to find the globally optimal configurations for $n = 16, 17, 18, 21, 22, 23$, which partly reflects the difficulty of this problem when n grows. In our opinion the failures in [19] (cf [22]) were caused mainly by high potential barriers between solutions with different

0305-4470/98/031035+13$19.50

numbers of points on the disk boundary; later in this paper we try to overcome this difficulty by systematically choosing initial solutions with a different number of charges on the disk boundary, see section 2.2.

Munera [18] and Queen [16] both restricted the structure of the configurations to consist of concentric rings of charges. The energy of a configuration is usually insensitive to the precise angular coordinates of charges [16], thus the optimal configurations are found by assigning a suitable number of charges on the periphery of each concentric ring and then finding the radii of the rings that minimize the potential energy. Munera [18] failed to find the optimal solutions for $n = 17, 19, 20$ and the energy for $n = 18$ was inaccurate. Queen [16] applied this approach more successfully and found conjecturally optimal configurations for $n \leqslant 17$ and $n = 29, 30$. The difficulty in this approach is to decide how many concentric rings to use and how many charges to assign to each ring. Furthermore, in view of the results in this paper, when n is sufficiently large, the concentric 'rings' are not always exactly circular in an equilibrium configuration.

Since [22] no more tables or figures of (conjecturally) optimal charge configurations have been published. In this work we will partially fill that gap in the literature by presenting a number of conjecturally optimal, or conjectural *ground-state* configurations of up to 37 charges and the best configurations found of up to 80 charges. We expect the vast majority of these configurations to also be optimal.

The optimization methods that we have used can be classified as probabilistic global optimization methods [23], which cannot *guarantee* that the best solutions found are globally optimal. We must bear in mind that the number of variables in many problem instances of this paper is relatively high, thus we cannot expect that the current deterministic global optimization methods can solve this problem completely.

It appears that when the number of charges is increased there are many local optima with high potential barriers between them. An outline for a catastrophe theoretical model relating different locally optimal configurations has been presented in [24].

1.2. Related problems

A related problem of packing charges on the surface of a sphere (or equivalently, in the sphere [6]) has been studied for a longer time, and it is known as Thomson's problem [25]. For Thomson's problem many extensive tables exist in the literature. The first computer search for stable configurations was performed in the 1950s by Cohn [26]. A few configurations were discussed in [27]. More solutions were published in the 1980s [18, 28–30], but the most extensive tables have appeared in the last few years [31–36]. As so often when trying to find global optima in a difficult multimodal optimization problem, several conjectured global optima have turned out to be only local optima, see for example [31, 37, 38]. Some authors restrict the solutions, or sometimes just the initial solutions, to have certain symmetries [18, 33], in which case the optimization problem may be significantly easier. But if the globally optimal configuration does not have such a required symmetry, then it cannot be found by that kind of a method. Examples can be found by comparing [18, 30, 39]. Hardin, Sloane and Smith are preparing a book on spherical codes, and they also maintain tables containing the best currently known solutions to Thomson's problem. The tables are available on the World Wide Web through Neil Sloane's home page at ⟨URL:http://www.research.att.com/∼njas/⟩.

It is also possible to consider non-coulombic potentials when searching for optimal configurations in a sphere or on a circular disk [6, 9, 11, 40–44]. When the repulsion forces are central and only distance dependent, Leech [45] showed that on the surface of the sphere

the only configurations which are in equilibrium under all such laws of repulsion are those that have some rotational symmetry about every diameter through particles of the system, see also [27].

Other related problems are those of packing circles on a disk [46], on a sphere [47–49], or on a hypersphere [50]. Packing equal circles can be thought of as finding optimal configurations for sets of points with a repulsion force which increases very rapidly as the distance decreases, i.e. the shortest distance determines the potential energy of the system.

Physical experiments have been made with equal parallel cylindrical bar magnets on an air table [51], where the potential is slightly different, because instead of d^{-2} the repulsion force is proportional (to a considerable degree of accuracy) to

$$\frac{1}{d^2} - \frac{d}{(d^2+h^2)^{3/2}}$$

where h is the distance between the point poles of the supposedly rigid magnetic dipole and d is the distance between the magnets. As noted in [51], this problem was studied experimentally in the last century by Mayer. Experiments with small charged conductive balls were carried out in [52].

2. The optimization methods used in this work

We denote a point charge configuration in the plane by $C = \{\boldsymbol{p}_1, \boldsymbol{p}_2, \ldots, \boldsymbol{p}_n\}$, where the points lie on a circular disk of unit radius centred in the origin, i.e. $\|\boldsymbol{p}_i\| \leqslant 1$. The energy function to be minimized is

$$E(C) = \sum_{1 \leqslant i < j \leqslant n} \|\boldsymbol{p}_i - \boldsymbol{p}_j\|^{-1}. \tag{1}$$

This corresponds to minimizing the potential energy when there is a coulombic repulsion force between each pair of equal point charges.

Because (1) is a nonlinear, non-convex function, the problem of finding global optima can be very hard. A related, more general problem of determining the ground states of atom clusters with artificial central-body forces is NP-hard (non-deterministic polynomial-time hard) [53].

All the optimization algorithms that we have used in this work select a suitable set of initial solutions and then apply a local optimization algorithm to each solution. The algorithms described below can be regarded as probabilistic global optimization algorithms and they differ only in the selection of the initial solutions. In all the computations we have used a truncated Newton method TN/TNBC [54] as a local optimizer.

2.1. Algorithm A1: Multistart with initial solutions from the infinite case

In the first approach we simply take random initial solutions and perform a local optimization run for each solution; then we take the best solution found. This is the multistart algorithm.

When the number of charges n tends to infinity (it is assumed that the total charge is constant), the limit density of charges when the potential energy is minimized is

$$f(r) = \frac{K}{2\pi\sqrt{1-r^2}} \tag{2}$$

where K is the total charge on the disk and r is the distance from the centre of the unit radius disk [16]. In the first approach we take the random initial solutions from the distribution defined by $f(r)$.

Even this simple approach was able to find most of the configurations in section 3, including all of those in [22] that were not found in [19].

Using the results found with this approach we can further develop the selection of initial solutions. When selecting the initial solutions, the number of points near the disk boundary is crucial, because if a charge is caught on the boundary, a strictly descent [55] local optimization algorithm cannot push it back on the interior of the disk.

If we manage to estimate reasonably well the number of charges on the boundary in the optimal configuration, we can use an initial solution with that number of charges on the boundary, thus reducing the number of variables and speeding up the optimization process considerably.

2.2. Algorithm A2: Multistart with heuristic initial solutions

In the second approach we take the best configuration of n charges found so far and assume that the number of charges on the disk boundary (denote this by $\tilde{n}_0$) is approximately the same as in the (possibly still unknown) optimal configuration.

Now we form the initial solutions first by putting b, $\tilde{n}_0 - \delta \leqslant b \leqslant \tilde{n}_0 + \delta$, charges evenly spaced on the disk boundary, where δ is an integer constant reflecting our confidence in the quality of the solutions found so far. Then we distribute the remaining charges according to (2), when the number of the charges on the boundary is taken into account. In the computations we used $\delta = 6$; in no case the best configuration found (see section 3) had a greater deviation from $\tilde{n}_0$ than 2.

2.3. Algorithm A3: Multilevel single linkage

One weakness of the multistart algorithm is that it repeatedly performs optimization runs with initial solutions that are in the same region of attraction [55]. One way of overcoming this problem is to store the initial solutions and start a new optimization run only if no better initial solution has been sampled in the neighbourhood of the new initial solution. This idea has been developed into the *multilevel single linkage* (MLSL) algorithm [56].

As the third optimization approach in this paper we have used a reduced sample version of MLSL, which is depicted in figure 1. At each major iteration the algorithm takes N random charge configurations (with the same distribution as in algorithm A2) and calculates their energies, so in the kth round of the algorithm we have a total of kN random configurations. From these kN configurations we take the γkN best (lowest energy) configurations, where $0 < \gamma \leqslant 1$; these configurations are the *reduced sample*. For each configuration in the reduced sample we check if there is a better configuration at a distance which is less than or equal to the threshold r. If no such better configuration exists, we perform a local optimization run starting from the configuration in the reduced sample.

The threshold value r for deciding whether a configuration is 'near' another configuration is gradually decreased during the optimization run as the number of configurations is increased. Note that even if at one time a local optimization run is not started from a certain configuration, this decision may be revoked later when the threshold value has become smaller. It is necessary to store the results of the local optimization runs so that no more than one optimization run is applied to a single initial solution.

When using the standard Euclidean vector norm as the distance function between solutions, we can get very high distances between solutions that are essentially the same, obtained from each other by permuting the points and rotating or reflecting the configuration. This observation leads to the key idea in our adaptation of MLSL: we use a special heuristic

(1) Set $k := 0$, choose $N > 0$ and $0 < \gamma \leqslant 1$.
(2) Let $k := k + 1$.
(3) Add N random configurations to previously sampled initial solutions.
(4) Select $\gamma\, Nk$ lowest-energy configurations of all Nk configurations; this is the *reduced sample*.
(5) Apply local optimization from each configuration in the reduced sample except if there is another configuration with lower energy at a distance which is less than or equal to the threshold r.
(6) If the stopping condition is not satisfied, repeat from (2).

Figure 1. Multilevel single linkage algorithm.

distance function that tries to compensate the difficulties caused by different orientations of the solutions and different permutations of the points. Let us first consider different permutations of the points. We take two configurations, denote these by S and T, and for each point of the configurations we find the nearest neighbour in the other configuration. We define the distance function

$$d(S, T) = \sum_{i=1}^{n} \min_j \|\boldsymbol{s}_i - \boldsymbol{t}_j\|^2 + \sum_{i=1}^{n} \min_j \|\boldsymbol{t}_i - \boldsymbol{s}_j\|^2$$

which clearly equals 0 if S and T are obtained from each other by just permuting the points.

Now, two initial solutions S and T with the same number b of points on the disk boundary are compared by calculating the b rotations of S that make the boundary points coincide with those of T. Then we calculate the reflection of S, and after another n rotations we select the smallest distance between T and the rotations and reflections of S. Clearly, this approach gives distance 0 whenever S is a (possibly reflected) rotation of T. If S and T have a different number of points on the disk boundary, they are considered as having infinite mutual distance and thus the distance function partitions the solution space into disjoint subsets infinitely far from each other.

With our heuristic distance function the formula in [56, equation (2)] for critical distance r cannot be used directly. As the critical distance r between two solutions S and T we use

$$r = c\left(\frac{\log p}{p}\right)^{1/u} \tag{3}$$

where u is the number of variables and a suitable value for the constant c is determined experimentally. The number of sampled initial solutions in the solution space partition containing S and T is denoted by p—we keep a separate critical distance for each partition. If S and T are in different partitions, then they are considered as having infinite mutual distance and the value of r does not matter. Our method can be seen as if we were running an MLSL algorithm on each solution space partition in parallel, giving the computing resources to the most promising initial solutions. If there is only one partition, then (3) and equation (2) in [56] give the same critical distances for each iteration step when the value of c is selected suitably.

The problem of determining a suitable stopping criterion is a very hard problem in global optimization. We have simply limited the number of major iterations of MLSL and the number of local optimization runs; the algorithm stops when either of these limits is reached.

Table 1. Energies of the configurations.

n	E	n	E	n	E
12	59.575 675	35	672.342 18	58	2008.0682
13	71.807 362	36	715.068 32	59	2083.0334
14	85.347 290	37	759.342 75	60	2159.3584
15	100.220 96	38	804.920 00	61	2237.1926
16	116.452 00	39	851.911 30	62	2316.2518
17	133.816 52	40	900.118 72	63	2396.9504
18	152.477 90	41	949.851 58	64	2478.9810
19	172.494 82	42	1000.825 4	65	2562.5685
20	193.629 80	43	1053.304 5	66	2647.4781
21	216.179 11	44	1107.079 4	67	2733.9499
22	240.121 68	45	1162.330 4	68	2821.6862
23	265.201 04	46	1218.980 8	69	2910.8539
24	291.727 83	47	1277.007 0	70	3001.4558
25	319.665 51	48	1336.375 2	71	3093.5796
26	348.770 89	49	1397.200 9	72	3187.0854
27	379.353 32	50	1459.582 1	73	3281.8499
28	411.344 31	51	1523.209 2	74	3378.1982
29	444.547 75	52	1588.206 5	75	3475.8612
30	479.079 57	53	1654.657 8	76	3575.2077
31	514.917 13	54	1722.684 2	77	3675.7938
32	552.269 74	55	1791.973 7	78	3777.8992
33	590.806 30	56	1862.649 7	79	3881.4275
34	630.834 38	57	1934.738 5	80	3986.2335

3. Results

The lowest-energy configurations of 12–80 charges found during this research are depicted in figures 2–5.

The energies of the configurations are tabulated in table 1, where E is the energy of the configuration. The best previously published energies for configurations with $n \leqslant 23$, $n = 29, 30$ [16, 18, 19, 22] coincide with the values in our table. In [19] a figure of a configuration of 50 charges was shown, but the energy was not given. By visual inspection the configuration looks similar to the one in figure 3. No results have been previously published for other values of n.

Many of the configurations seem to have symmetries. However, since the optimization process can provide the coordinates of the points only with limited accuracy, it is difficult to say for certain from the numerical results directly when a configuration has a symmetry. It is not precluded that an optimal (or best currently known) configuration is only *almost* symmetrical. Such examples have been found in circle packings, see for example the packings of 36 and 53 circles in a circle [46]. In [46] the coordinates of each circle of the packing were solved numerically with very high precision before determining the symmetry group.

It would be very interesting to see how our MLSL approach works when the charges are confined in a sphere instead of a circular disk, but unfortunately the heuristic initial solutions and distance function cannot be easily extended to the case of a sphere.

When comparing the optimization algorithms of this paper we note that the multistart algorithm with heuristic initial solutions worked so well that it found all the configurations in figures 2–5 except the configuration of 55 charges, which was only found by MLSL. How-

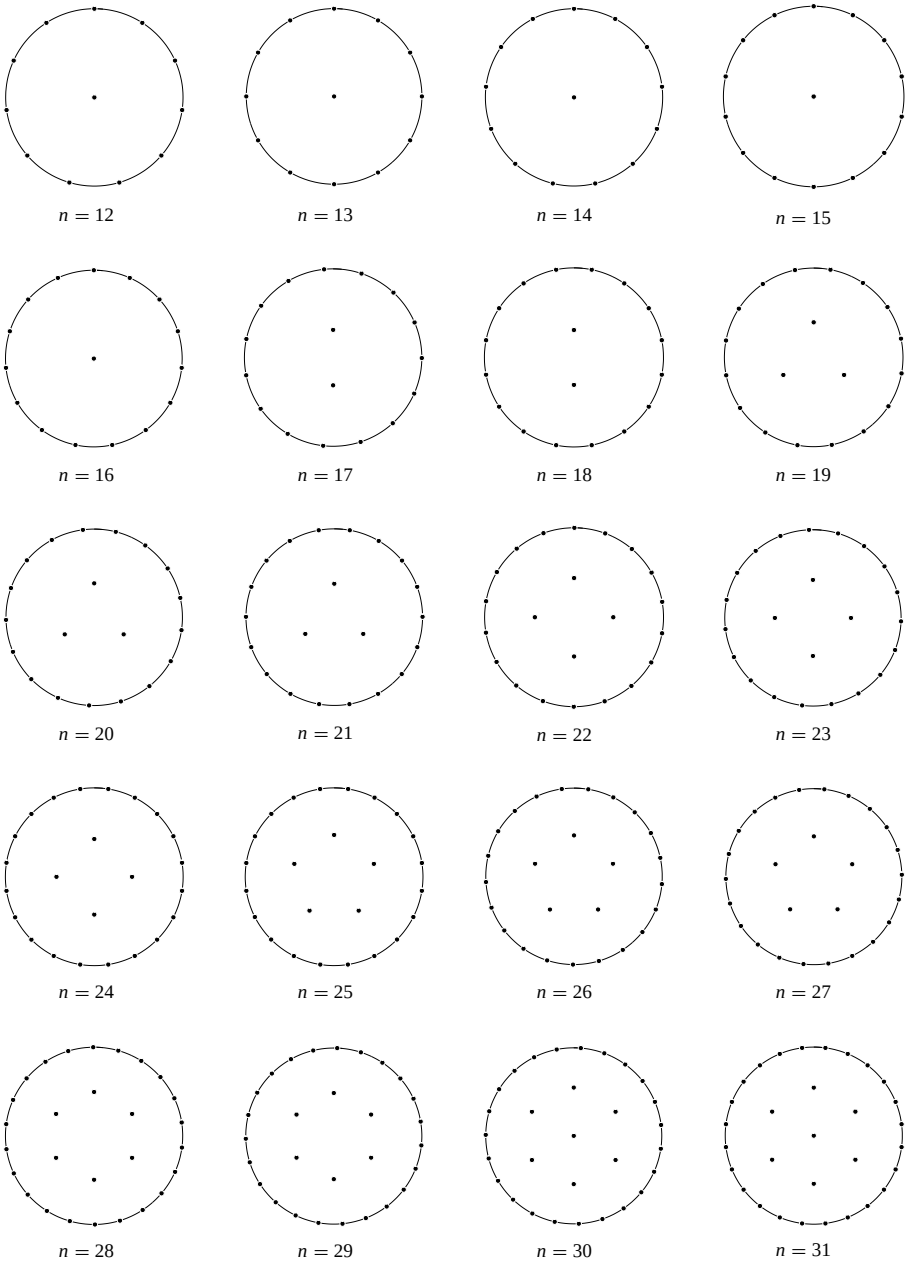

Figure 2. Configurations of 12–31 charges.

ever, fewer local optimization runs were needed when using MLSL, so it is clear that MLSL with a heuristic distance function is better when only a limited number of optimization runs can be performed. Our initial approach using multistart with initial solutions from the infinite case is clearly inferior to both of the more advanced approaches, but it is needed to provide an initial estimate for the number of charges on the disk boundary in the optimal case.

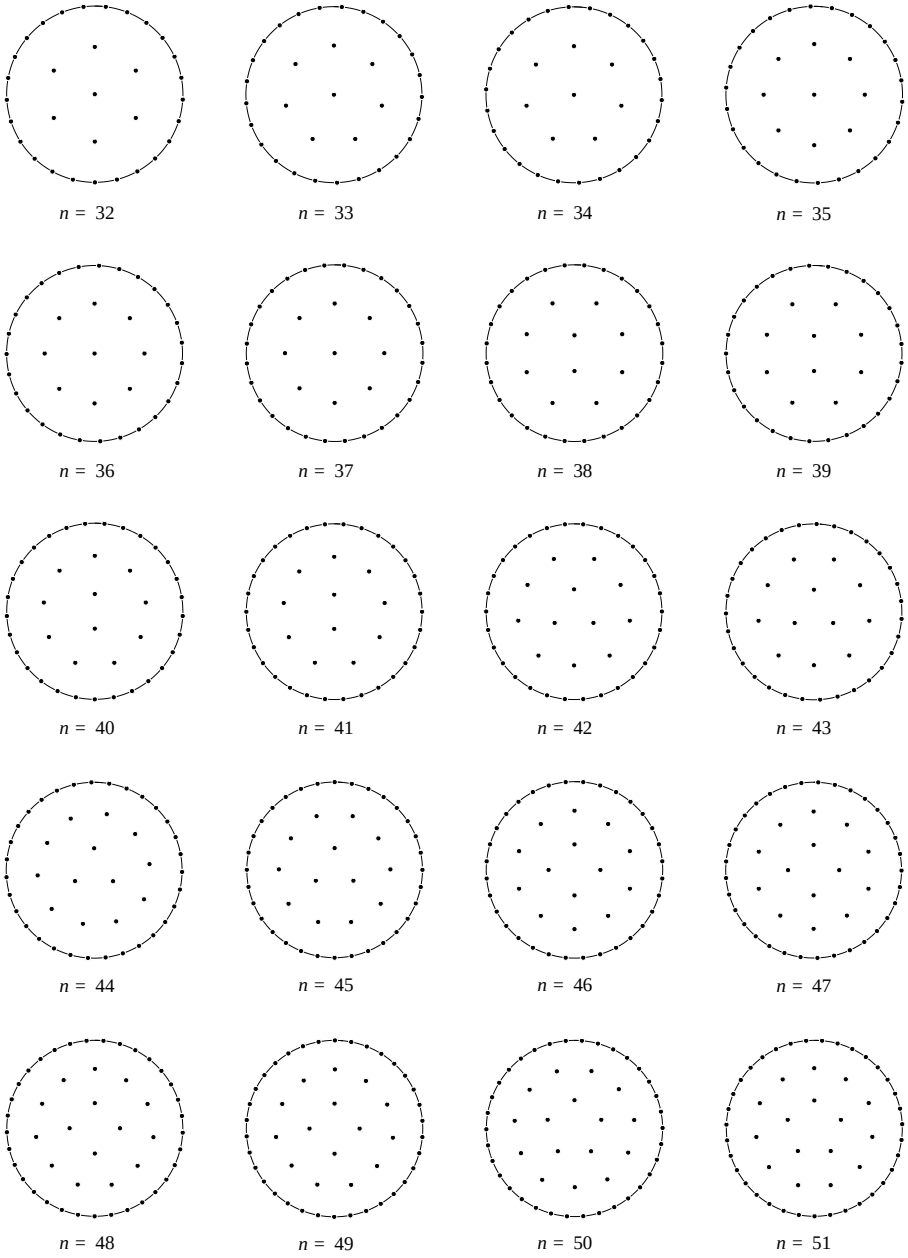

Figure 3. Configurations of 32–51 charges.

If the plane is filled with point charges with constant charge density, the hexagonal lattice is the lowest-energy configuration [57]. However, when the charges are confined to a bounded area, the shape of the area determines the structure of the optimal configurations. It has been supposed that the optimal configurations on a circular disk consist of charges arranged in concentric rings, charges spaced evenly on each ring [16, 19]. Approximately, this seems to be the case in the configurations of this work, as well. This observation can

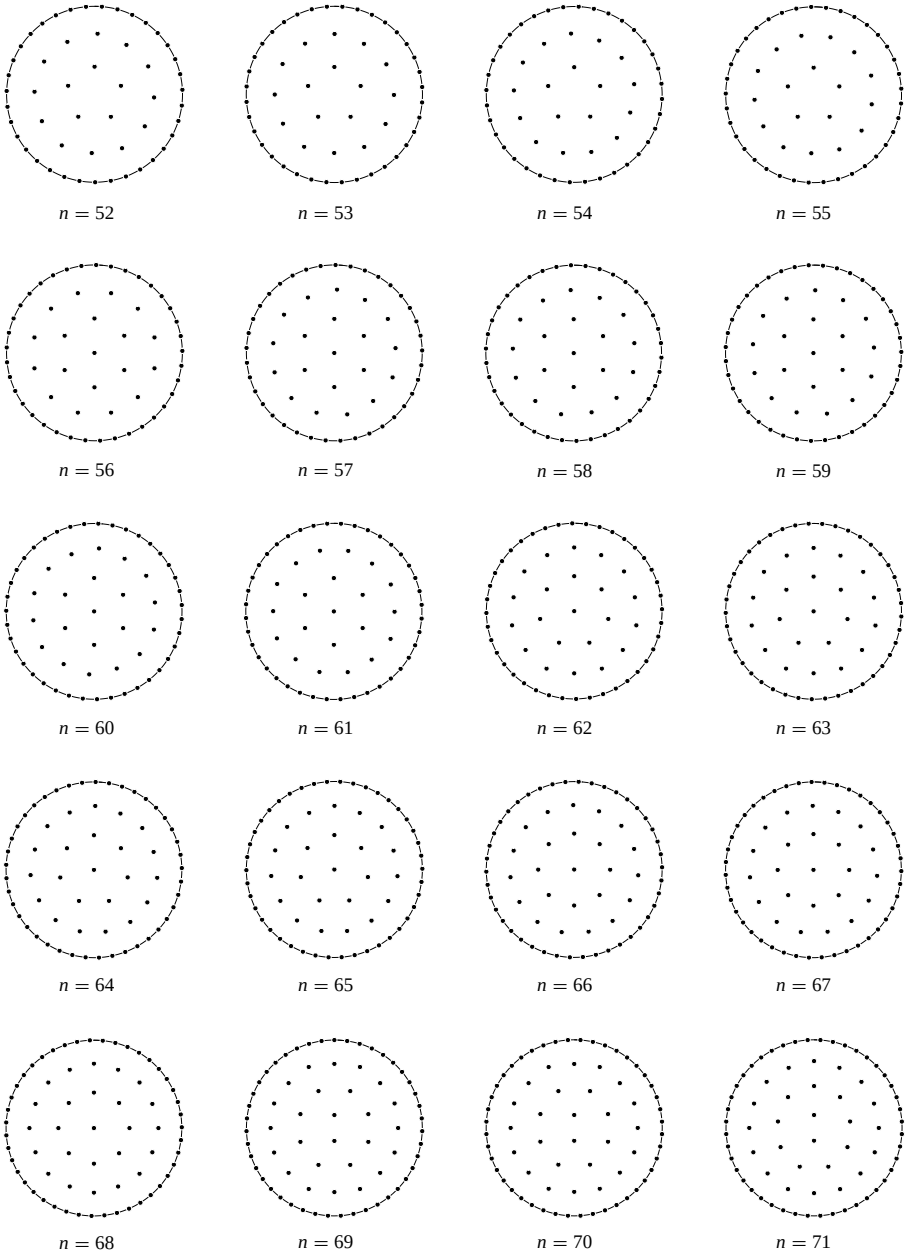

Figure 4. Configurations of 52–71 charges.

be used to construct special initial solutions consisting of a few concentric rings of charges [16, 22]. We have deliberately avoided this structure in the initial solutions, since it is not known how well this structure is preserved when n is increased.

It is interesting to find out which configurations in figures 2–5 are in equilibrium under *any* law of repulsion. To do this we prove a theorem analogous to that in [45]. By 'law of repulsion' we mean a repulsive force between two points that only depends on the distance

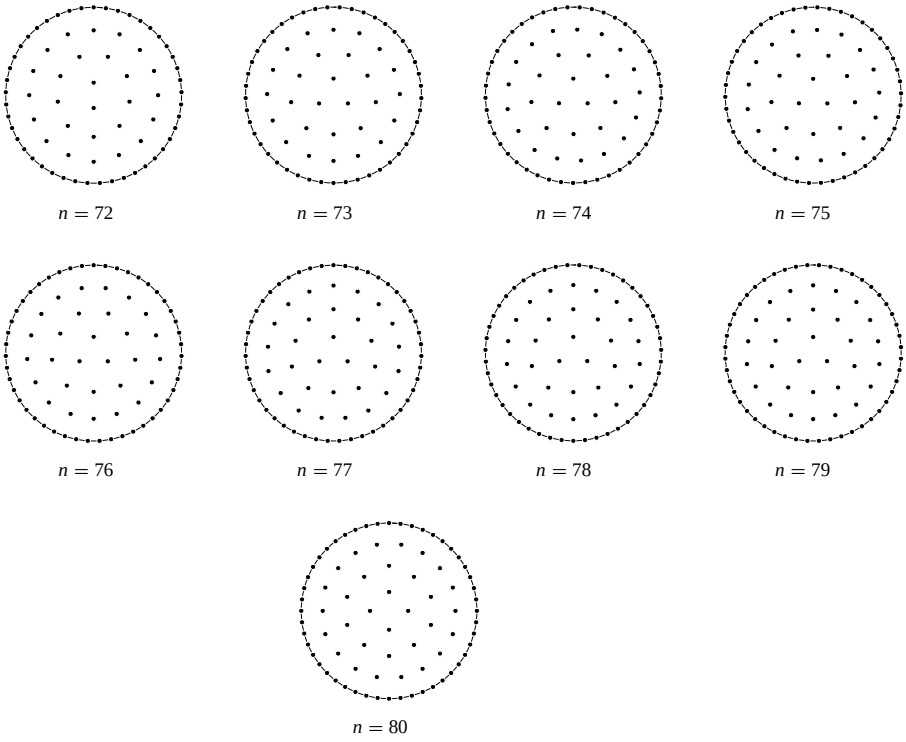

Figure 5. Configurations of 72–80 charges.

between the points, i.e. the magnitude of the force between $\boldsymbol{p}_i$ and $\boldsymbol{p}_j$ is $v(\|\boldsymbol{p}_i - \boldsymbol{p}_j\|)$, where $v(d)$ is any function such that $v(d) \geqslant 0$ for all $d \geqslant 0$.

Theorem 1. The configurations of $n \geqslant 2$ points on a circular disk that are in equilibrium under any law of repulsion are exactly:

(i) n points evenly spaced on the disk boundary, and

(ii) $n - 1$ points evenly spaced on the disk boundary and one point in the centre of the disk. In this case we require $n > 2$.

Proof. A configuration is in equilibrium if and only if each of the points is in equilibrium, i.e. the resultant of the repulsive forces on the point is zero, or the point is on the disk boundary and the resultant is perpendicular to the tangent of the disk boundary at that point.

Assume for the rest of the proof that we have a configuration that is in equilibrium under any law of repulsion and thus all points are in equilibrium whatever the repulsion law may be.

The first part of the proof will show that there can be at most one point in the interior of the disk and if it exists, it must be located in the centre of the disk. Let us assume that there is a point $\boldsymbol{p}$ not on the disk boundary. Now all the other points must be on one or more concentric circles centred in $\boldsymbol{p}$, we call these circles *shells*.

We can take the shell s with the greatest radius r around $\boldsymbol{p}$. This shell must clearly contain at least two points, because otherwise $\boldsymbol{p}$ would not be in equilibrium (take a potential function $v(d) = 1$, if $d = r$ and $v(d) = 0$ otherwise). Furthermore, if we take any 180°

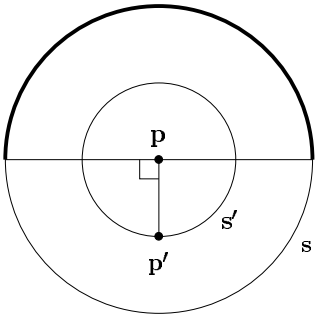

Figure 6. First part of proof.

arc of the shell, it must contain at least one point. Now, suppose there were another shell around $\boldsymbol{p}$ apart from s, denote this shell by s'. This shell s' contains by definition at least one point $\boldsymbol{p}'$ (see figure 6). As noted before, there must be at least one point on the 180° arc of s directly across $\boldsymbol{p}'$ (shown as the heavy curve in figure 6). It follows that $\boldsymbol{p}'$ must have a shell s'' with radius r'' such that $r'' > r$, and because all the points are confined in s, there must be an empty arc greater than 180° on s''; thus $\boldsymbol{p}'$ is not in equilibrium under all repulsion laws.

Hence, if there is a point $\boldsymbol{p}$ in the interior of the disk, then there must be at least two other points and they must all lie on a single circle whose centre coincides with $\boldsymbol{p}$. Furthermore, this circle must coincide with the disk boundary, otherwise the points on it could not be in equilibrium under coulombic repulsion force.

As the second step we show that the points on the disk boundary must be evenly spaced. As shown before, there must be at least two points on the boundary. We take two points on the boundary with the smallest mutual distance, let them be $\boldsymbol{b}_1$ and $\boldsymbol{b}_2$. Now if there is a point in the centre of the disk, it cannot contribute any tangential force to the points on the boundary, so there must be a point $\boldsymbol{b}_3$ located on the boundary on the other side of $\boldsymbol{b}_2$ such that $\|\boldsymbol{b}_1 - \boldsymbol{b}_2\| = \|\boldsymbol{b}_2 - \boldsymbol{b}_3\|$. If such $\boldsymbol{b}_3$ does not exist, then $\boldsymbol{b}_2$ is not in equilibrium under repulsion force that varies according to $v(d) = 1$ when $d = \|\boldsymbol{b}_1 - \boldsymbol{b}_2\|$ and $v(d) = 0$ otherwise. Similarly we can infer the existence of $\boldsymbol{b}_4, \boldsymbol{b}_5, \ldots$ until $\boldsymbol{b}_i = \boldsymbol{b}_1$ for some i.

We have now shown that no such configuration that is in equilibrium under all repulsion laws exists except possibly the two types mentioned in theorem 1. By symmetry considerations it is clear that all those configurations are in equilibrium under any potential that depends only on the distance between points. □

Using the theorem we find out that the best configurations of $n \leqslant 16$ charges are equilibrium configurations under any law of repulsion. They are also locally optimal circle packings, but of them only the configurations of up to six charges, all of type 1 in theorem 1, are at the same time globally optimal circle packings (see [46] and its references). When $n = 6$ there exists another globally optimal packing of circles that is not a globally optimal charge configuration. We conjecture that the optimal circle packings and charge configurations are different for all $n > 6$.

Acknowledgment

The research was supported by the Vilho, Yrjö and Kalle Väisälä Foundation and the Academy of Finland.

References

[1] Berezin A A 1985 *Nature* **315** 104
[2] Janssen J E M and Melissen J B M 1993 *SIAM Rev.* **35** 643
[3] Melissen J B M and Schuur P C 1993 *SIAM Rev.* **35** 643–4
[4] Richberg R 1993 *SIAM Rev.* **35** 644–5
[5] Webb S 1985 *Nature* **316** 302
[6] Calkin M G, Kiang D and Tindall D A 1987 *Am. J. Phys.* **55** 157–8
[7] Aspden H 1986 *Nature* **319** 8
[8] Aspden H 1987 *Am. J. Phys.* **55** 199
[9] MacGowan D 1985 *Nature* **315** 635
[10] Naumann R A 1985 *Nature* **316** 302
[11] Calkin M G, Kiang D and Tindall D A 1986 *Nature* **319** 454
[12] Berezin A A 1985 *Nature* **317** 208
[13] Berezin A A 1986 *Chem. Phys. Lett.* **123** 62–4
[14] Rees M 1985 *Nature* **317** 208
[15] Nityananda R 1985 *Nature* **316** 301
[16] Queen N M 1985 *Nature* **317** 208
[17] Cormack A M 1985 *Nature* **316** 301–2
[18] Munera H A 1986 *Nature* **320** 597–600
[19] Wille L T and Vennik J 1985 *J. Phys. A: Math. Gen.* **18** L1113–17
[20] Wille L T 1986 *Nature* **324** 46–8
[21] Wille L T 1987 *Nature* **352** 374
[22] Wille L T and Vennik J 1986 *J. Phys. A: Math. Gen.* **19** 1983
[23] Törn A and Žilinskas A 1989 *Global Optimization* (Berlin: Springer)
[24] Berezin A A 1991 *Phys. Scr.* **43** 111–15
[25] Whyte L L 1952 *Am. Math. Monthly* **59** 606–11
[26] Cohn H 1956 *Math. Tables Aids Comput.* **10** 117–20
[27] Melnyk T W, Knop O and Smith W R 1977 *Can. J. Chem.* **55** 1745–61
[28] Ashby N and Brittin W E 1986 *Am. J. Phys.* **54** 776–7
[29] Frickel R H and Bronk B V 1987 *Can. J. Chem.* **66** 2161–5
[30] Webb S 1986 *Chem. Phys. Lett.* **129** 310–14
[31] Altschuler E L, Williams T J, Ratner E R, Dowla F and Wooten F 1994 *Phys. Rev. Lett.* **72** 2671–4
[32] Edmundson J R 1991 *Acta Cryst.* A **48** 60–9
[33] Edmundson J R 1993 *Acta Cryst.* A **49** 648–54
[34] Erber T and Hockney G M 1991 *J. Phys. A: Math. Gen.* **24** L1369–77
[35] Glasser L and Every A G 1992 *J. Phys. A: Math. Gen.* **25** 2473–82
[36] Weinrach J B, Carter K L and Bennett D W 1990 *J. Chem. Educ.* **67** 995–9
[37] Altschuler E L, Williams T J, Ratner E R, Dowla F and Wooten F 1995 *Phys. Rev. Lett.* **74** 1483
[38] Erber T and Hockney G M 1995 *Phys. Rev. Lett.* **74** 1482
[39] Webb S 1986 *Nature* **323** 20
[40] Kogan I, Perelomov A M and Semenoff G W 1992 *Phys. Rev.* B **45** 12 084–7
[41] Berezin A A 1986 *J. Math. Phys.* **27** 1533–6
[42] Berezin A A 1987 *Am. J. Phys.* **55** 199
[43] Bergersen B, Boal D and Palffy-Muhoray P 1994 *J. Phys. A: Math. Gen.* **27** 2579–86
[44] Van de Waal B W 1988 *Am. J. Phys.* **56** 583–4
[45] Leech J 1957 *Math. Gaz.* **41** 81–90
[46] Graham R L, Lubachevsky B D, Nurmela K J and Östergård P R J 1997 Dense packing of congruent circles in a circle *Discrete Math.* to appear
[47] Conway J H and Sloane N J A 1993 *Sphere Packings, Lattices and Groups* (New York: Springer)
[48] Kottwitz D A 1991 *Acta Cryst.* A **47** 158–65

[49] Nurmela K J 1995 *Report* A32, Digital Systems Laboratory, Helsinki University of Technology
[50] Wille L T 1987 *J. Phys. A: Math. Gen.* **20** L1211–18
[51] Pescetti D and Piano E 1988 *Am. J. Phys.* **56** 1106–9
[52] Blonder G E 1985 *Bull. Am. Phys. Soc.* **30** 403
[53] Wille L T and Vennik J 1985 *J. Phys. A: Math. Gen.* **18** L419–22
[54] Nash S G 1984 *SIAM J. Numer. Anal.* **21** 770–88
[55] Rinnooy Kan A H G and Timmer G T 1987 *Math. Programming* **39** 27–56
[56] Rinnooy Kan A H G and Timmer G T 1987 *Math. Programming* **39** 57–78
[57] Bonsall L and Maradudin A A 1977 *Phys. Rev.* B **15** 1959–73